Synthesis, characterization, structures, and DFT study of zinc(II) complexes with tributylphosphine chalcogenides

Zied Gouid,[a,b] M.A.K. Sanhoury,[a,c]* R. Ben Said,[b] Cameron L. Carpenter-Warren,[d] Alexandra M.Z. Slawin,[d] M.T. Ben Dhia,[a] J. Derek Woollins,[d] S. Boughdiri[b]

[a] *Laboratory of Structural Organic Chemistry: Synthesis and Physicochemical Studies, Department of Chemistry, Faculty of Sciences of Tunis, University of Tunis El Manar, 2092, Tunis, Tunisia*

[b] *Research Unit: Physico-Chimie des Matériaux à l'Etat Condensé, Department of Chemistry, Faculty of Sciences of Tunis, University Tunis El Manar, Tunis, 2092,Tunis, Tunisia*

[c] *Research Unit in Materials Chemistry, Faculty of Sciences and Techniques, UNA, Nouakchott, Mauritania*

[d] *EaStCHEM School of Chemistry, University of St Andrews, St Andrews, Fife KY16 9ST, UK*

Abstract

Four new zinc(II) complexes of the type $[ZnCl_2(n\text{-}Bu_3PE)_2]$ (E = O (**1**), S (**2**), Se (**3**) or Te (**4**)) have been synthesized from zinc(II) chloride and the ligands $n\text{-}Bu_3PE$ giving yields of 56-88%. The adducts were characterized by multinuclear (^{31}P, ^{13}C and ^{77}Se) NMR, conductivity, IR spectroscopy and by X-ray analyses. The zinc complexes **1**–**4** are comprised of two ligands coordinated to the metal centre in a distorted tetrahedral arrangement. The P=E bond lengths of 1.497(7) (E = O), 2.000(4) (E = S) and 2.178(2)Å (E = Se) in these complexes are slightly elongated compared to those in the free ligand. In addition, a DFT/B3LYP theoretical study on the geometry optimization of the title ligands and their zinc complexes has been carried out in order to support and complement the experimental data and to further investigate the nature of the chalcogenide-metal interaction. The results show good agreement between the experimental and theoretical data.

Keywords: Phosphine chalcogenide, zinc(II) complex, structural study, NMR, DFT/B3LYP.

1. Introduction

The coordination chemistry of phosphine chalcogenides R_3PE (E = O, S, Se) has attracted considerable attention due to their ease of preparation, high solubility and good reactivity towards different metal ions in many organic solvents [1-9]. They were among the first chalcogenide sources used in colloidal nanocrystal syntheses and remain one of the most common precursors

[10]. For instance, there has been a renewed interest in the metal complexes of this class of compounds in light of their increasing use as suitable single-source precursors for the production of binary metal chalcogenide thin films ME (M = Zn, Cd or Hg; E = S, Se or Te) as well as ME quantum dots [11,12].

On the other hand, studies into the coordination chemistry of R_3PE (E= O, S, Se and Te) towards the same metal would be very informative as to the nature of metal-ligand interactions upon complex formation [13] as well as to the mechanism of P-E cleavage in the complex following activation in the synthesis of related metal chalcogenide nanocrystals [14]. The intermediate Lewis acidity of zinc which could favour complex formation with both hard (E = O) and soft (E = S, Se or Te) ligands, especially zinc chloride, and its wide use in colloidal ME quantum dots [15, 16] make it the metal of choice for such studies. In addition, most of the ligands used as capping agents in ME nanocrystal synthesis are trialkylphosphine oxides in particular the bulkier isolating trioctylphosine oxide (TOPO) and to a lesser extent tributylphosphine oxide (TBPO). The capping agent is then substituted with a smaller ligand such as pyridine upon formation of a more optically efficient hybrid system [17]. Recently, we have shown that the fabrication of the less bulky TBPO-capped CdSe and ZnSe nanoparticles-organic polymer hybrid system does not require the capping agent substitution step, yielding comparable efficiency to that containing pyridine as the surfactant [18, 19]. As some metal complexes could be used as single source precursors for the preparation of such nanoparticles, the synthesis and investigation of the chemistry of new related metal complexes would be of particular interest. To our surprise, no zinc(II) chloride complexes with tributylphosphine chalcogenides were reported, which could be due to both the hygroscopic nature and tedious coordination chemistry of this zinc salt [20].

In continuation of our previous works on metal complexes with phosphine chalcogenides [21-23], we describe herein the synthesis and characterization of new zinc(II) chloride complexes with tributylphosphine chalcogenides (n-Bu_3P=E: E = O, S, Se or Te) using multinuclear (^{13}C, ^{31}P and ^{77}Se) NMR, IR spectroscopy, conductivity measurements, X-ray analysis and DFT/B3LYP theoretical calculations.

2. Experimental details

2.1. General experimental procedures

Zinc chloride anhydrous (≥99.9%) and ethanol puriss (≥99.8%) were used as received from the commercial supplier (SIGMA-ALDRICH). All preparations were carried out under nitrogen in solvents dried by standard techniques [24] and stored over molecular sieves. All NMR spectra were recorded on a Bruker AC-300 instrument in $CDCl_3$ as solvent, ^{31}P at 121 MHz (85% H_3PO_4), ^{1}H at 300 MHz, ^{13}C at 75,4 MHz ^{77}Se at 57.2 MHz (Me_2Se) and IR spectra YL 2000 FT-IR Spectrometer.

The conductivity measurements were carried out for 10^{-3} M solutions of the complexes dissolved in acetonitrile (dried on molecular sieves). Tributylphosphine was commercially supplied and purified by vacuum distillation before use. The ligands n-$Bu_3P(E)$ was prepared according to methods described in literature [25-28].

2.2. Preparation of complexes

To a solution of zinc chloride (1 mmol, 0.13 g) in 50 mL of ethanol was added n-$Bu_3P(E)$ (2 mmol) (E = O: 0.43 g; S: 0.47 g; Se: 0.56 g and Te: 0.66 g) in anhydrous dichloromethane (5 mL). The reaction mixture was stirred at room temperature for 12 h and concentrated in vacuo. Addition of anhydrous hexane and cooling for 24 h led to the precipitation of the complex, which was washed with the same solvent and vacuum dried for several hours.

[$ZnCl_2$(n-$Bu_3PO)_2$]. White solid, yield = 0.48 g (84%). M.p. = 89.4 °C. ^{1}H NMR (300 MHz, $CDCl_3$, 25°C): δ = 0.87 (t, 18H, $^{3}J^{1}_{H}$-$^{1}_{H}$ = 6.8Hz), 1.35 (m, 12H), 1.44 (m, 12H), 1.81 ppm (m, 12H). ^{13}C NMR (75.4 MHz, $CDCl_3$, 25 °C): δ = 13.39 (s), 23.38 (d, $^{3}J_{P-C}$ = 19.6 Hz), 23.92 (d, $^{2}J_{P-C}$ = 6.7 Hz), 26.31 ppm (d, $^{1}J_{P-C}$ = 65.6 Hz). IR: 2974, 2947, 2885 1468, 1119 (νP=O), 1074 cm^{-1}. Λ_M = 13 Ω^{-1} cm^2 mol^{-1}. Anal. Calcd. For [$ZnCl_2$(n-$Bu_3PO)_2$]: C, 50.31; H, 9.50 %. Found C, 50.96; H, 10.26%.

[$ZnCl_2$(n-$Bu_3PS)_2$]. White solid, yield = 0.28 g (47%) ^{1}H NMR (300 MHz, $CDCl_3$, 25°C): δ = 0.80 (t, 18H, $^{3}J^{1}_{H}$-$^{1}_{H}$ = 7.1 Hz), 1.32 (m, 12H), 1.48 (m, 12H), 2.10 ppm (m, 12H). ^{13}C NMR (75.4 MHz, $CDCl_3$, 25 °C): δ = 12.53 (s), 23.00 (d, $^{3}J_{P-C}$ = 16.6 Hz), 23.48 (d, $^{2}J_{P-C}$ = 4.52 Hz), 27.46 ppm (d, $^{1}J_{P-C}$ = 49.0 Hz). IR: 2976, 2948, 2885, 1469, 1099, 563 cm^{-1} (νP=S). Λ_M = 37 $\Omega^{-1}cm^2$ mol^{-1}. Anal. Calcd. For [$ZnCl_2$(n-$Bu_3PS)_2$]: C,47.64; H, 9.00 %. Found C, 46.95; H, 9.21 %.

[$ZnCl_2$(n-$Bu_3PSe)_2$]. White solid, yield = 0.40 g (58%) M.p. = 79.4 °C. ^{1}H NMR (300 MHz, $CDCl_3$, 25°C): δ = 0.91 (t, 18H, $^3J^1_{H-}{}^1_H$ = 7.3 Hz) 1.40 (m, 12H), 1.50 (m, 12H), 2.19 ppm (m, 12H). ^{13}C NMR (75.4MHz, $CDCl_3$, 25 °C): δ = 13.6(s), 23.62 (d, $^3J_{P-C}$ = 16.6 Hz), 24.93 (d, $^2J_{P-C}$ = 4.52 Hz), 27.84 ppm (d, $^1J_{P-C}$ = 42.2 Hz). IR: 2974, 2945, 2884, 1467, 1093, 482 cm^{-1} (νP=Se). Λ_M = 20 Ω^{-1} cm^2 mol^{-1}. Anal. Calcd. For [$ZnCl_2$(n-$Bu_3PSe)_2$]: C, 41.25; H, 7.79 %. Found C, 40.85.; H, 8.02 %.

[$ZnCl_2$(n-$Bu_3PTe)_2$]. Yellow solid, yield = 0.28 g (38%). ^{1}H NMR (300 MHz, $CDCl_3$, 25°C): δ = 0.97 (t, 18H, $^3J^1_{H-}{}^1_H$ = 9.6 Hz), 1.50 (m, 12H), 1.57 (m, 12H), 2.18 ppm (m, 12H). IR: 2975, 2947, 2885, 1469, 1125, 467 cm^{-1} (νP=Te). Anal. Calcd. For [$ZnCl_2$(n-$Bu_3PTe)_2$]: C, 36.21; H, 6.84 %. Found C, 35.58; H, 6.82 %.

2.3.X-Ray structural details

X-ray analyses for **1** and **2** were performed using a Rigaku Sealed tube generator and a Saturn 724 detector at 125 K and for **3** using a Rigaku FRX (dual port) rotating anode/confocal optic high brilliance generator with Dectris P200 detectors, and an OxfordCryostream Cobra accessory at -180(1) C. All data were collected with Mo Kα radiation (k = 0.71073 Å) and corrected for Lorentz and polarisation effects. The data for all of the compounds were collected and processed using CrystalClear (Rigaku) [29]. The crystal structures were solved using direct methods [30] or heavy atom Patterson methods [31] and expanded using Fourier techniques [32]. The non-hydrogen atoms were refined anisotropically and hydrogen atoms were refined using the riding model. All calculations were performed using CrystalStructure [33] crystallographic software package and SHELXL-97 (Table 1) [34]. **2** This structure was determined using Mo radiation, so the Flack parameter shows errors; there is considerable disorder in the R groups. We did examine the data for twinning and see no evidence of this. For **3** there are large voids in the structure We examined the difference map carefully and can find no significant peaks which could be modelled. This data was collected on a very small crystal The WGHT parameter reflects that rather than any lack of modelling in the refinement

Table 1

2.4. Computational details

Density functional theory (DFT) calculations were carried out on the complexes and their ligands using the Gaussian 09 suite of programs [35], with the hybrid functional B3LYP [36] along with the 6-31G* basis set. The geometries of the complexes and their ligands were optimized using analytical gradient. The optimization was unrestrained and vibrational frequencies were used to

characterize the stationary points as minima. Several local configurations near the achieved energy minimum were examined. As the renewed optimizations converged to the same molecular geometry, we believe the achieved energy minimum to be the global one.

3. Results and discussion

3.1. Synthesis

The reaction of zinc chloride in ethanol solution with the ligands produces the complexes $[ZnCl_2L_2]$. These were purified by washing in anhydrous hexane to give the pure complexes as white or yellow solids that are soluble in dichloromethane, chloroform, acetonitrile and nitromethane, and insoluble in hexane. Complex **4** is the least stable and decomposes within 24 h at room temperature liberating elemental tellurium but more stable when kept at lower temperatures (0 to -10 °C).

The molar conductance of the complexes in acetonitrile (10^{-3} M) shows values between 13 to 37 Ω^{-1} cm^2 mol^{-1}, indicating that these chloride complexes are nonelectrolytes. These results show that the complexes are adducts in good agreement with our previous results obtained with other metals [23]. The choice of zinc(II) chloride over the bromide or iodide was based on two purposes; to maintain the intermediate character of zinc(II) and obtain complexes that could be more soluble in organic solvents which would allow NMR studies in solution. The differences observed between found and calculated values in the elemental analysis data are due to the high air sensitivity of the complexes, especially the telluride derivative **4**.

3.2. Spectroscopic characterization

The complexes were characterized by IR and multinuclear (^{1}H, ^{13}C, ^{31}P, ^{77}Se) NMR spectroscopy. The IR spectra (Table 2) show that the stretching vibration of the P=E band is shifted to lower frequencies as compared to those of free ligands. This shift is more pronounced for the P=O stretching frequency compared to the corresponding ν(P=S), ν(P=Se) and ν(P=Te) absorptions. This is reasonable since the vibrations involving the relatively heavy tellurium, selenium and sulfur atoms would be less sensitive to coordination than those with the lighter phosphorus or oxygen atoms. The results are in a good agreement with those reported for similar complexes [37], confirming that the metal-ligand interaction is more important in the case of the oxide ligand compared to the sulfide, selenide and Telluride ligands ($\Delta\nu$ is 38, 32, 29 and -7 cm^{-1} for P=O, P=S, P=Se and P=Te derivatives, respectively). The lack of shifts in the IR spectrum for the

characteristic $\nu_{P=Te}$ band in complex **4** could be due to the low sensitivity of the heavier Te atom to coordination charges.

The ^{31}P NMR spectra of complexes were obtained at room temperature and the data are listed in Table 2. These spectra show signals that are shifted downfield compared to those of the free ligands, confirming the coordination of the tributylphosphine chalcogenide ligand with zinc through the P=E group.

In the case of the selenide, the complexation showed also a decrease in the magnitude of $^{1}J_{P-Se}$ coupling constant. Such a change is attributed to coordination of P=Se to the metal atom through selenium through metal–selenium bonding. However no P-Te coupling ($^{1}J_{P-Te}$) is observed for the telluride complex (**4**) at room temperature. The lack of observable $^{1}J_{P-Te}$ in this complex could be attributed to a faster ligand exchange compared to that occurring in the selenide complex. The difference in the ^{31}P chemical shift between free and bound ligands ($\Delta^{31}P$) is more important in complexes with Bu_3PO ligand (14.2 ppm) than that observed in zinc complexes with Bu_3PS (4.2 ppm), Bu_3PSe (4.3 ppm) and Bu_3PTe (3.8 ppm) (Table 2), consistent with the above mentioned IR data. Furthermore, complex formation also influenced the C-P carbon nuclei as indicated by ^{13}C NMR, revealing that the oxide derivative is affected in a different manner to that of other chalcogenides (Table 2). Since the metal used is unchanged ($ZnCl_2$), there appears to be a correlation between the hardness of the ligand donor atom (E) and the coordination chemical shift of the ligands. This would indicate a decrease in the magnitude of the metal-ligand interaction of the ligands towards zinc along the series $Bu_3PO >> Bu_3PS \geq Bu_3PSe > Bu_3PTe$, suggesting a more substantial complex dissociation down the series.

Table 2

3.3. Structural study

To elucidate the constitution of the complexes formed, as well as to provide a clear understanding of the effect of ligand structure on the stereochemistry of these complexes, we examined the solid state structure of the complexes $[ZnCl_2(n\text{-}Bu_3PE)_2]$ with E = O, S and Se. Due to the instability of complex **4**, no suitable crystals could be obtained for this derivative. The geometries of complexes **1-3** (Figs. 1-3) are similar; the only difference being the nature of the chalcogen atom. Two chalcogenide atoms of the two R_3PE ligands and two chloride ions coordinate to Zn and the geometry around the metal center can be described as being on distorted tetrahedral (Fig.1). Table 3 lists important bond lengths and angles.

Table 3

The P-E bond lengths of 1.515(6), 1.497(7) for P=O, 2.000(4),1.998(4) for P=S and 2.160(2), 2.178(2) Å for P=Se are typical for P=E double bonds. The average P=E bond distances are all shorter than the sum of the representative covalent radii of P and E atoms, implying some retention of π bonding in the complex. However, these P=E distances are longer than those observed in the free ligands [38,39], indicating that the P=E bond is weakened upon complex formation with the singly bonded structure becoming more pronounced down the period [40] with an increasing dipole moment a long the series +P−O− < +P−S− < +P−Se− < +P−Te− [41, 42]. Moreover, the structures of these complexes reveal that while the average P-O-Zn is 131.0(4), 132.9(4)°, those of P-S-Zn (108.26(15),109.19(14)°) and P-Se-Zn (102.4(7), 108.6(7)°) are smaller than 109°. This suggests that the latter could be classified as π donors, employing P-E π bonding electrons for donation, rather than σ non-bonding electrons (lone pairs) used for coordination in the oxide derivative, in fair agreement with the bonding model proposed by Burford *et al.* [13]. The Zn–E bonds show distances of 1.980(6),1.952(6); 2.376(3), 2.356(3) and 2.509(13),2.515(12) Å for oxide, sulfide and selenide derivatives, respectively (Table 3). These are longer than the sum of covalent radii for representative single P-E bonds but much shorter than the sum of van der Waals radii [43]. The effect is being more important down the series, in good agreement with the order obtained from our IR and NMR data for the magnitude of metal-ligand interaction. The average P-C distances in the complexes are 1.798, 1.808, and 1.804 Å for oxide, sulfide and selenide derivatives which are shorter than in corresponding ligands [38, 39]. Finally, Zn-Cl bond distances (range 2.227(3)-2.261(2) Å) are also shorter than the sum of covalent radii (2.3Å). We examined the structures for intermolecular interactions and found no unusual packing/intermolecular contacts of note.

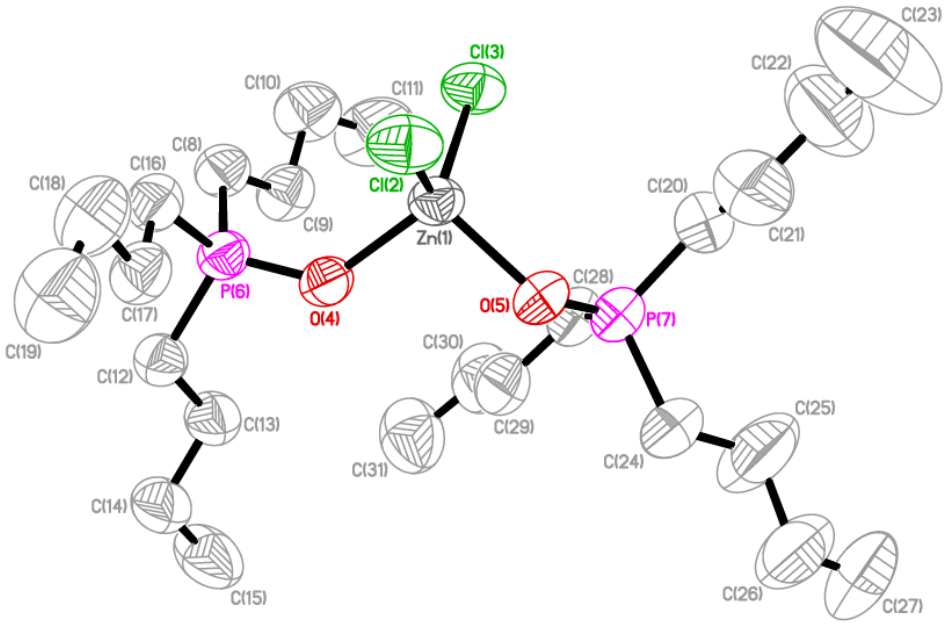

Fig 1: An ORTEP diagram of the first molecule of complex 1 in the asymmetric unit (Z'=2), showing all non-H atoms with thermal ellipsoids at 50 % probability and all H atoms have been omitted for clarity.

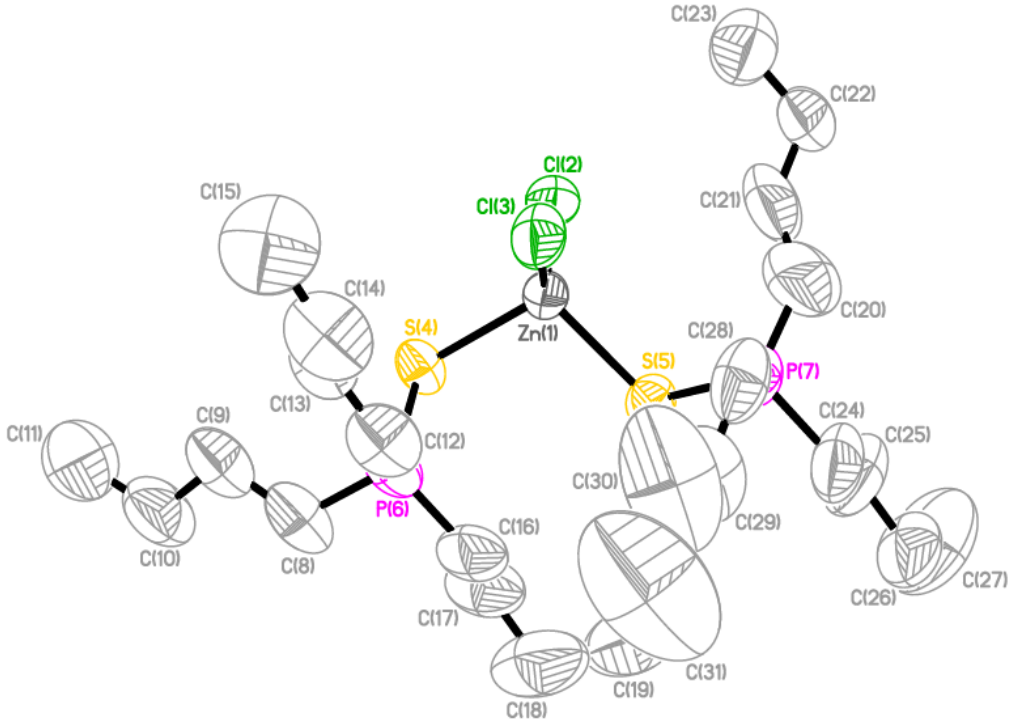

Fig 2: An ORTEP diagram of the first molecule of complex 2 in the asymmetric unit (Z'=2), showing all non-H atoms with thermal ellipsoids at 50 % probability and all H atoms have been omitted for clarity.

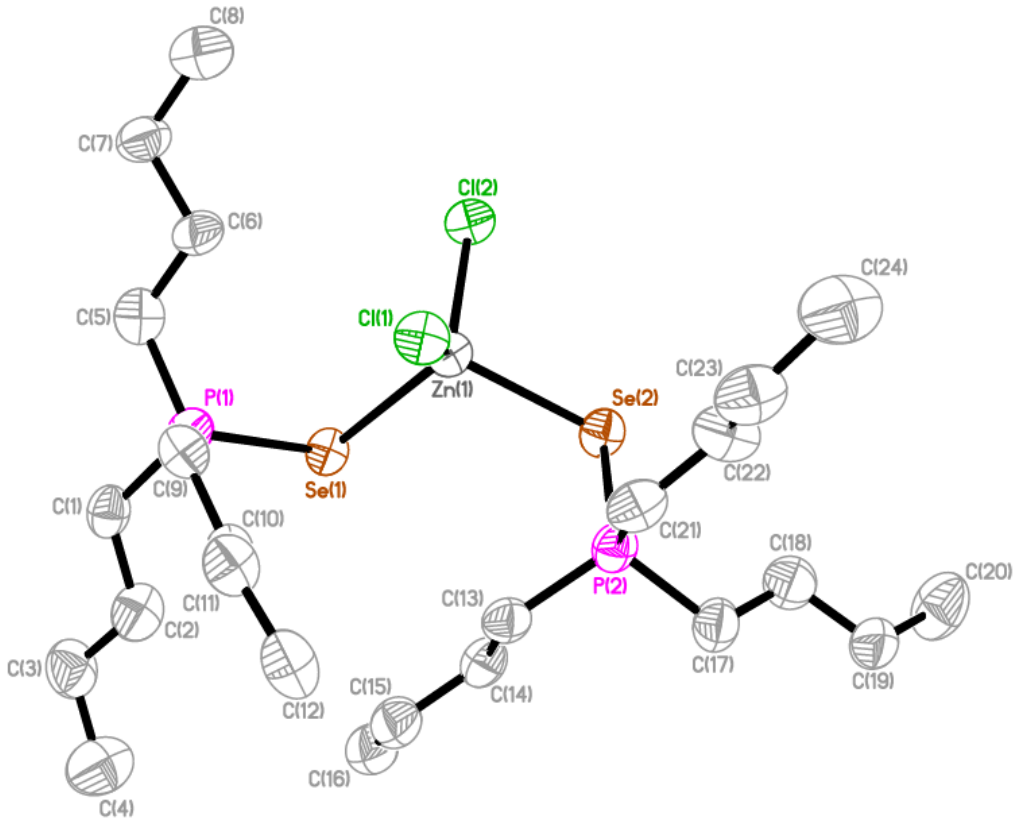

Fig 3: An ORTEP diagram of complex 3, showing all non-H atoms with thermal ellipsoids at 50 % probability and all H atoms have been omitted for clarity.

3.4. Theoretical calculations

To shed more insight into the structures of the complexes prepared and further confirm the experimental data, the geometries of ligands and their complexes were optimized by means of DFT method using B3LYP functional. The appropriate structure of the compound was confirmed as energy minima by calculating the vibrational frequency and confirming the absence of any imaginary frequencies. The DFT/B3LYP optimized values of selected geometrical parameters of the ligands and their complexes are listed in Table 4.

In the complexes, the coordination mode is confirmed by a lengthening of the P=E bond compared to that of the free ligands calculated at the same level of theory. This lengthening is consistent with the low stretching frequency observed in the IR spectra and may also explain the differences observed in the ^{31}P NMR chemical shifts between the free and bond ligands in solution. The lengthening of the P=E bonds in the complexes is also accompanied by a shortening of the P-C bonds compared to that in the free ligands, consistent with the X-Ray data. The changes in bond distance are also supported in solution for complex **3** by an observed decrease in $^{1}J_{P\text{-}Se}$ coupling

constant value compared with that in the free ligand. These results are in good agreement with the values reported for similar compounds [44]. The Zn-Cl bond of $[ZnCl_2(n\text{-}Bu_3PE)_2]$ (2.278, 2.259, 2.259 and 2.257Å for E = O, S, Se and Te, respectively) shows also a lengthening compared to that of the free zinc chloride (2.081 Å) calculated at the same level of theory.

The Zn-E-P angle shows, as expected, a more bent structure for telluride (94.5°), selenide (97.8°) and sulfide (104°) complexes than in the oxide (128.4°) analog (Table 4), in general agreement with experimental X-ray data and with trends usually observed for chalcogenide derivatives [41]. The results thus obtained for the complexes show both a longer P=E bond distance and a decrease in Zn-E-P bond angle when the size of the chalcogen increases along the series: P=O < P=S < P=Se < P=Te. The difference in details between the crystallographically determined values and theoretically calculated ones is presumably due to crystal packing effect in the former.

Table 4

In addition, it seems interesting to compare the experimental IR spectra with those theoretically found with DFT calculations. The calculated ν(P=O) stretching vibrations of ligands and their complexes are listed in Table 5.

Table 5

As obtained experimentally, the DFT calculated P=E stretching vibrations in the complexes show a lower frequency shift compared to that of the free ligands calculated at the same level of theory, in agreement with the lengthening of the P=E bond upon complexation with zinc. The difference in the P=E frequency shift $\Delta\nu_{P=E}$ decreases in the order P=O > P=S > P=Se > P=Te. These results further confirm that the P=O bond is the most affected upon complexation, suggesting that the mode of bonding of this bond with the metal (σ bonded) would be different than those in other chalcogenides (π bonded) as shown above. This is in good agreement with our experimental IR data.

4. Conclusions

New zinc complexes with tributylphosphine chalcogenides were prepared and fully characterized by multinuclear (^{13}C, ^{31}P and ^{77}Se) NMR, IR, X-ray analysis and DFT theoretical calculation techniques. The experimental NMR, IR and X-ray data show that P=E bond distances are weakened upon complex formation and the P-E-Zn bond angles decreases down the period E = O > S > Se > Te. Such a trend was further confirmed with theoretical DFT/B3LYP geometry

calculations. This could be very useful in understanding the mode of bonding of phosphine chalcogenides in their metal complexes and the mechanism of P-E cleavage upon activation in the synthesis of metal chalcogenide nanocrystals from related complexes. The use of complexes 2-4 as single source precursors for the preparation of zinc chalcogenide nanoparticles is underway in this laboratory**.**

Acknowledgement
We are grateful to the Tunisian Ministry of High Education and Scientific Research for financial support (LR99ES14) of this research.

Appendix A. Supplementary data

CCDC 1564126, 1564127 and 1564128 contains the supplementary crystallographic data for complexes **1-3**, respectively. These data can be obtained free of charge via http://www.ccdc.cam.ac.uk/conts/retrieving.html, or from the Cambridge Crystallographic Data Centre, 12 Union Road, Cambridge CB2 1EZ,
UK; fax: (+44) 1223-336-033; or e-mail: deposit@ccdc.cam.ac.uk.

References

[1] C.M. Mikulski, J.S. Skryantz, N.M. Karayannis, L.L. Pytlewski, L.S. Gelfand. *Inorg. Chim. Acta*., **27**, 69-73 (1978).

[2] N.M. Karayannis, C.M. Mikulski, L.L. Pytlewski*, Inorg. Chim. ActaRev*., **5**,69 (1971).

[3] K. Issleib, B. Mitscherling. *Z.anorg. allg. Chem*., **304**, 73 (1960).

[4] F.A. Cotton, E. Bannister. *J. Chem. Soc.*, 1873 (1960).
E. Bannister, F.A. Cotton. *Ibid*., 1878 (1960).

[5] D.M.L. Goodgame, F.A. Cotton. *Ibid*., 2298-3735 (1961).

[6] A.M. Brodie, S.H. Hunter, G.A. Rodley. C.J. Wilkins. *J. Inorg. Chim. Acta*., **2**, 195 (1968).

[7] N.M. Karayannis, C.M. Mikulski, L.L. Pyrlewski. *J. Inorg. Chim. Acta. Rev*., **5**, 69 (1977).

[8] L. Qu, Z. Peng, X. Peng. *Nano Lett.,* **1**, 333−337 (2001)

[9] J. Jasieniak, C. Bullen, E.J. Van, P. Mulvaney. *J. Phys. Chem. B.*, **109**, 20665−20668 (2005).

[10] K. Bania, N. Barooah, J.B. Baruah. *Polyhedron.*, **26,** 2612−2620 (2007).

[11] (a) M. Afzall, D. Crouch, M.A. Malik, M. Motevalli, P. O'Brien, J.-H. Park, J.D. Woollins.

Eur. J. Inorg. Chem., 171 (2004).

(b) J. Waters, D.J. Crouch, J. Raftery, P. O'Brien. *Chem. Mater*., **16**, 3289 (2004), and refs therein.

[12] T. Chivers, J.S. Ritch, S.D. Robertson, J. Konu, H.M. Tuononen. *Acc. Chem. Res*., **43**, 1053 (2010), and refs therein.

[13] N. Burford, B.W. Royan, R.E.v.H. Spence, R.D. Rogers. J. *Chem. Soc. Dalton Trans*., 2111– 2117 (1990) and all references.

[14] R.G. Rodríguez, M.P. Hendricks, B. M. Cossairt, H. Liu, J.S. Owen. *Chem. Mater*., **25**, 1233- 1249 (2013).

[15] H. Shen, H. Wang, X. Li, J.Z. Niu, H.X. Chen, L.S. Li. *Daltron Trans*., 10534-10540 (2009).

[16] C.S. Tiwary. P. kunbhakar, A.K. Mitra, K. Chattopadhyay. *Journal of Luminescence*., **129**, 1366-1370 (2009).

[17] See for example: E.S. Williams, K.J. Major, A. Tobias, D. Woodall, V. Morales, C. Lippincott, P.J. Moyer, M. Jones. *J. Phys. Chem. C.*, **117**, 4227−4237 (2013).

[18] A. Benchaabane, Z. Ben Hamed, M.A. Sanhoury, F. Kouki, A. Zeinert, H. Bouchriha. *Appl. Phys. A.,* **122**, 1–10 (2016).

[19] N. Mastour, Z. Ben Hamed, A. Benchaabane, M.A. Sanhoury, F. Kouki. *Org. Electron.,* **14**, 2093–2100 (2013).

[20] T.S. Lobana, R. Hundal, P. Turner. *J. Coord. Chem*., **53**, 301-309 (2001).

[21] R. Mallek. M.A.K. Sanhoury. M.T. Ben Dhia. M.R. Khaddar. *J. Coord. Chem*., **67**, 1541-1549 (2014).

[22] R. Mallek. M.A.K. Sanhoury. L. Bahri. M.R. Khaddar. M.T. Ben Dhia. *J. Coord. Chem*., **69**, 726-734 (2016).

[23] M.A. Sanhoury, T. Mbarek, A.M.Z. Slawin, M.T. Ben Dhia, M.R. Khaddar, J.D. Woollins. *Polyhedron.,* **119** 106–111 (2016).

[24] D.D. Perrin, W.L.F. Armarego. *Purification of Laboratory Chemicals*, 6th Edn, Butterworth-Heinemann, Oxford (2009).

[25] C.R. Hilliard, N. Bhuvanesh, J.A. Gladysz, J.Blumel. *Dalton Trans.,* **41**, 1742-1754 (2012).

[26] D.J. Peterson, H.R. Hays. *J. Org. Chem*., **30**, 1939-1942 (1965).

[27] S. Franks, F.R. Hartley, D.J.A. McCaffery. *J. Chem. Soc., Perkin I*., **302**, 3033 (1979).

[28] S.A. Buckler, *J. Amer. Chem. Soc*., **84**, 3093-3096 (1962).

[29] (a) CrystalClear 1.6, *Rigaku Corporation*, (1999).

(b) CrystalClear Software User's Guide, Molecular *Structure Corporation*, (2000).;

(c) J.W. Pflugrath, ActaCrystallogr. D Biol. *Crystallogr.,* **55**, 1718 (1999).

[30] SIR97: A. Altomare, M. Burla, M. Camalli, G. Cascarano, C. Giacovazzo, A. Guagliardi, A. Moliterni, G. Polidori, R. Spagna. *J. Appl. Crystallogr*., **32**, 115 (1999).

[31] PATTY: P.T. Beurskens, G. Admiraal, H. Behm, G. Beurskens, J.M.M. Smits, C. Smykalla, Z. Kristallogr., (Suppl. 4) 99 (1991).

[32] DIRDIF99: P.T. Beuerskens, G. Admiraal, G.Beuerskens, W.P. Bosman, R. deGelder, R. Israel, J.M.M. Smits, The DIRDIF-99 program system, Technical Report of the Crystallography Laboratory, University of Nijmegen, The Netherlands, (1999).

[33] (a) CrystalStructure 3.8.1: Crystal Structure Analysis Package, Rigaku and Rigaku/MSC (2000–2006). 9009 New Trails Dr. The Woodlands, TX 77381 USA.

(b) CrystalStructure 4.0: Crystal Structure Analysis Package, RigakuCorporation (2000–2010). Tokyo 196–8666, Japan.

[34] G.M. Sheldrick, ActaCrystallogr., Sect. A: Fundam. Crystallogr., **64**. 112 (2008).

[35] M.J. Frisch, G.W. Trucks, H.B. Schlegel, G.E. Scuseria, M.A. Robb, J.R. Cheeseman, G. Scalmani, V. Barone, B. Mennucci, G.A. Petersson, H.Nakatsuji, M. Caricato,X. Li, H.P. Hratchian, A.F. Izmaylov, J. Bloino, G. Zheng, J.L. Sonnenberg, M. Hada, M. Ehara, K. Toyota, R. Fukuda, J. Hasegawa, M. Ishida, T. Nakajima, Y. Honda, O. Kitao, H.Nakai, T. Vreven, J.A.Montgomery Jr., J.E. Peralta, F.Ogliaro, M.Bearpark, J.J. Heyd, E. Brothers, K.N. Kudin, V.N. Staroverov, R. Kobayashi, J. Normand, K. Raghavachari, A. Rendell, J.C. Burant, S.S. Iyengar, J. Tomasi, M. Cossi, N.Rega, J.M. Millam, M. Klene, J.E. Knox, J.B. Cross, V. Bakken, C. Adamo, J. Jaramillo, R. Gomperts, R.E. Stratmann, O. Yazyev, A.J. Austin, R. Cammi, C. Pomelli, J.W. Ochterski, R.L. Martin, K. Morokuma, V.G. Zakrzewski, G.A. Voth, P. Salvador, J.J.Dannenberg, S. Dapprich, A.D. Daniels, O. Farkas, J.B. Foresman, J.V. Ortiz, J. Cioslowski, D.J. Fox, Gaussian 09 W Revision A. 02, Gaussian, Inc., Wallingford, CT, 2009.

[36] (a) A.D. Becke, *J. Chem. Phys*., **98**, 5648 (1993).

(b) C. Lee, W. Yang, R.G. Parr, *Phys. Rev*., **B 37**, 785 (1988).

[37] M.Mathew, G.J.Palenik., *Can.J.Chem*., **47**, 1093 (1969).

[38] (a) C.R. Hilliard, N. Bhuvanesh, J.A. gladysz, J. Blumel., *Dalton Tans*., **41**. 1742-1757 (2012).

[39] (b) J. Beckmann. E. Lork. O. Mallow. *Main Group Met. Chem*., **35**. 187–188 (2012).

[40] R Davies. Handbook of chalcogen chemistry: New perspectives in sulfur, selenium and tellurium; The Royal Society of Chemistry: 286−343 (2007).

[41] T. Lobana, S. Prog. *Inorg. Chem*., **37**, 495−581 (1989).

[42] R. Davies, C. Francis, A. Jurd, M. Martinelli, A. White, D. Williams, *Inorg. Chem*., **43**. 4802−4804 (2004).

[43] J.E. Huheey, E.A. Keiter, R.L. Keiter (Editors) *Inorganic Chemistry-Principles of Structure and Reactivity, 4th edn., Harper Collins College Publishers*, London, (1993).

[44] B.K. Santra, B.J. Liaw, C.M. Hung, C.W. Liu. *Inorg. Chem*., **42**, 26 (2003).

Table 1: Crystal data, data collection and refinement parameters for complexes **1-3**.

	1	**2**	**3**
Compound	$[ZnCl_2(Bu_3PO)_2]$	$[ZnCl_2(Bu_3PS)_2]$	$[ZnCl_2(Bu_3PSe)_2]$
Empirical formula	$C_{24}H_{54}Cl_2O_2P_2Zn$	$C_{24}H_{54}Cl_2S_2P_2Zn$	$C_{24}H_{54}Cl_2Se_2P_2Zn$
Formula weight (g/mol)	572.92	605.04	698.84
Crystal system	Orthorhombic	Orthorhombic	Orthorhombic
Space group	P n a 21	P n a 21	P b cn
a (Å)	21.6620(15)	22.3161(15)	25.317(2)
b (Å)	13.2995(9)	15.3340(10)	13.8476(13)
c (Å)	22.4803(15)	19.7230(13)	39.310(3)
α, β, γ (˚)	90.0	90.0	90.0
V ($Å^3$)	6476.4(8)	6749.1(8)	13781(2)
Z	8	8	16
Crystal shape, color	Prism, colorless	Prism, colorless	Prism, colorless
Crystal size (mm)	0.21, 0.20, 0.16,	0.33, 0.27, 0.16	0.10, 0.10, 0.05
Dcalc (Mg/m^3)	1.175	1.191	1.347
Absorption coefficient (mm^{-1})	1.039	1.123	3.085
F (0 0 0)	2464	2592	5760
Data	11777	12362	12705
Goodness-of-fit on F^2	0.894	1.020	0.980
Final R indices ($I > 2\sigma(I)$)	0.0560	0.0612	0.0692
R indices (all data)	0.0944	0.0902	0.1058
wR2	01357	016662	0.1682

Table 2: NMR (δ/ppm and J/Hz) and IR (v(P=E)/cm^{-1}) data for the complexes **1**-**4**.

	^{31}P		^{77}Se		$^{1}J_{P-Se}$		v(P=E)	
Ligand	L	Complex ($\Delta^{31}P$)[a]	L	Complex ($\Delta^{77}Se$)[b]	L	Complex ($\Delta\ ^{1}J_{P-Se}$)[c]	L	Complex (Δv(P=E))[d]
Bu_3PO	48.9	63.1 (14.2)	-	-	-	-	1157	1119 (38)
Bu_3PS	48.6	52.8 (4.2)	-	-	-	-	595	563 (32)
Bu_3PSe	36.7	41.0 (4.3)	384.0	311.3(72.7)	685	578 (107)	511	482 (29)
Bu_3PTe	-13.2	-9.34 (3.8)					460	467 (-7)

a) $\Delta\delta^{31}P = |\delta^{31}P(complex) - \delta^{31}P(ligand)|$.

b) $\Delta\delta^{77}Se = |\delta^{77}Se(complex) - \delta^{77}Se(ligand)|$.

c) $\Delta^{1}J_{P-Se} = |^{1}J_{P-Se}(ligand) - {}^{1}J_{P-Se}(complex)|$.

d) Δv(P=E) | $v_{(P=E)}$ligands - $v_{(P=E)}$(complex)|.

Table 3: Selected bond lengths and angles for $[ZnCl_2(n\text{-}Bu_3PE)_2]$ (E = O (**1**), S (**2**) and Se (**3**).

	1	**2**	**3**		**1**	**2**	**3**
Zn-E1	1.980(6)	2.376(3)	2.509(13)	Cl1-Zn-E1	108.42(19)	98.66(10)	111.9(7)
Zn-E2	1.952(6)	2.356(3)	2.515(12)	Cl2-Zn-E2	107.7(2)	115.31(9)	110.6(7)
Zn-Cl1	2.238(3)	2.256(3)	2.250(2)	Cl1-Zn-Cl2	115.29(9)	114.92(12)	116.2(9)
Zn-Cl2	2.236(2)	2.227(3)	2.261(2)	Zn-E1-P1	131.0(4)	109.19(14)	102.4(7)
E1-P1	1.515(6)	1.998(4)	2.160(2)	Zn-E2-P2	132.9(4)	108.26(15)	108.6(7)
E2-P2	1.497(7)	2.000(4)	2.178(2)				

Table 4: DFT/B3LYP/6-31G* optimized geometrical and experimental parameters for complexes (**1**-**4**) [a]**.**

(a) Distances (Å) and angles (°)

		Theor.		Exp.	
		L	Complex	L	Complex
$Bu_3P=O$	P=E	1.507	1.538	1.489 [b]	1.506
	P-C	1.847	1.837	1.798 [b]	1.798
	Zn-E		1.984		1.966
	Zn-Cl		2.278		2.237
	Zn-E-P		128.4		131.9
	E-Zn-Cl		106.6		108.0
$Bu_3P=S$	P=E	1.979	2.030		1.999
	P-C	1.857	1.847		1.808
	Zn-E		2.469		2.366
	Zn-Cl		2.259		2.241
	Zn-E-P		104.0		108.7
	E-Zn-Cl		110.8		106.9
$Bu_3P=Se$	P=E	2.117	2.178		2.178
	P-C	1.860	1.847		1.804
	Zn-E		2.452		2.515
	Zn-Cl		2.259		2.261
	Zn-E-P		97.8		102.4
	E-Zn-Cl		115.4		111.2
$Bu_3P=Te$	P=E	2.407	2.436	2.368 [c]	
	P-C	1.856	1.851	1.828 [c]	
	Zn-E		2.702		
	Zn-Cl		2.257		
	Zn-E-P		94.5		
	E-Zn-Cl		105.8		

(b) and (c) from refs [37] and [38], respectively.

Table 5: DFT/B3LYP/6-31G* calculated and experimental ν(P=E) (cm^{-1}) data for ligands and their complexes.

	Ligand		Complex (Δν(P=E))	
	Exp	Theor	Exp	Theor
n-Bu_3PO	1157	1186	1119 (38)	1090 (96)
n-Bu_3PS	595	591	563 (32)	614 (28)
n-Bu_3PSe	511	563	482 (29)	541(22)
n-Bu_3PTe	460	481	467 (-7)	507 (-26)

Figure captions

Fig. 1. The X-ray crystal structure of $[ZnCl_2(Bu_3PO)_2]$ (**1**). All hydrogen atoms have been omitted for clarity.

Fig. 2. The X-ray crystal structure of $[ZnCl_2(Bu_3PS)_2]$ (**2**). All hydrogen atoms have been omitted for clarity.

Fig. 3. The X-ray crystal structure of $[ZnCl_2(Bu_3PSe)_2]$ (**3**). All hydrogen atoms have been omitted for clarity.